LIMNOLOGY
and
OCEANOGRAPHY: METHODS

Limnol. Oceanogr.: Methods 8, 2010, 462–473

The Underwater Vision Profiler 5: An advanced instrument for high spatial resolution studies of particle size spectra and zooplankton

Marc Picheral[1], Lionel Guidi[2], Lars Stemmann[1], David M. Karl[2], Ghizlaine Iddaoud[1], and Gabriel Gorsky[1]*

[1]Université Pierre et Marie Curie-Paris6, Laboratoire d'Océanographie de Villefranche, 06230 Villefranche-sur-Mer, France; CNRS, Laboratoire d'Océanographie de Villefranche, 06230 Villefranche-sur-Mer, France

[2]Center for Microbial Oceanography: Research and Education, University of Hawaii, Department of Oceanography, Honolulu, HI 96822 USA

Abstract

The Underwater Vision Profiler (UVP) was developed to quantify the vertical distribution of macroscopic particles and zooplankton > 100 µm in size. The smaller size limit is fixed by optical resolution, whereas the larger size limit is determined by the volume of water illuminated per image. The new fifth generation instrument (UVP5) is compact (30 kg in air) and operates either as a stand-alone instrument with an independent power supply for use on a mooring or free-drifting array, or as a component of a Conductivity, Temperature, and Depth (CTD)-rosette package. Images are recorded at a frequency up to 6 Hz. If the UVP5 is interfaced with a CTD, these images are acquired and analyzed in real time. Images are recorded every 20 cm at the 1 m s^{-1} lowering speed. The current maximum deployment depth is 3000 m. The recorded volume per image is 1.02 L, and the conversion equation from pixel area to size in mm^2 is $S_m=0.003S_p^{1.3348}$ where S_p is the surface of the particle in pixels and S_m the surface in mm^2. Comparisons between the earlier UVP versions and UVP5 indicate that images ranging in size from 105 µm to 2.66 mm are identical so historical and contemporary data sets can be compared.

A comprehensive understanding of the distribution, abundance, and dynamics of particulate matter and organisms in pelagic environments is crucial to predicting the export and sequestration of biogenic carbon. The existence of thin (cm to m) layers of marine snow aggregates, phytoplankton, and zooplankton (Alldredge et al. 2002) indicates that the pelagic ecosystem is very structured. Therefore, measurements of particles and organisms made at sampling frequencies that are compatible with other standard oceanographic instruments hold enormous potential for revealing factors that regulate distribution and abundance patterns.

Relatively few off-the-shelf instruments allow in situ measurements of oceanic particles. The LISST (Laser In Situ Scattering and Transmissometry; Sequoia Scientific; Karp-Boss et al. 2007) is a self-contained instrument that estimates the size of the particles based on scattering intensity. The LOPC (Laser Optical Plankton Counter; Herman 2004) records a shape approximation of objects crossing the light beam. Because they do not record images of the objects, the LISST and LOPC cannot distinguish among various classes of particles. Furthermore, the acquisition rate and the sampling volume of the LISST limit the accuracy of the size distribution for particles larger than 100 µm, and the resolution of the LOPC sensor array reduces the precision of the measurements for objects below 500 µm. Additionally, the LOPC sampling funnel may disrupt fragile aggregates, thereby altering their in situ characteristics.

More recently, several instruments that employ image analysis to characterize and enumerate oceanic particles have been developed and field tested (Benfield et al. 2007). These include (1) Video Plankton Recorder (VPR; Davis et al. 1992; Davis et al. 2005), (2) SIPPER (Samson et al. 2001), (3) ISIIS (Cowen and Guigand 2008), (4) ZOOVIS (Benfield et al. 2007),

*Corresponding author: Phone: 33 4 93 76 38 08; Fax: 33 4 93 76 38 34

Acknowledgments

The different UVP models were constructed at the Laboratoire d'Océanographie de Villefranche sur mer, France (UPMC/CNRS) with the support of the CNRS (Centre National de la Recherche Scientifique) LEFE-CYBER program, ZOOPNEC and the ANR POTES programs. Data used in this work were obtained during the BOUM cruise supported by CNRS. L. Guidi and D. M. Karl received financial support from the National Science Foundation (C-MORE) and the Gordon and Betty Moore Foundation. This study was supported by the SESAME IP of the European Commission's Sixth Framework Programme, under the priority Sustainable Development, Global Change and Ecosystems. Contract No. GOCE-2006-036949. Thanks to Thierry Moutin, Chief scientist during the BOUM experiment, Marsh Youngbluth for constructive discussions and Louis Legendre for encouragement of our technological development.

DOI 10.4319/lom.2010.8.462

(5) Flowcam (Sieracki et al. 1998), (6) Cytobuoy (Dubelaar and Gerritzen 2000), and (7) VPR (Dennett et al. 2002). The VPR has proven its efficacy (Dennett et al. 2002), but the large numbers of unfocused objects required intensive processing. These instruments still require specific cable or underwater interfacing and support for their deployment preventing their broad use. The FlowCam and the Cytobuoy pump water through the imaging cell and disturb the in situ size distribution of imaged objects (Karp-Boss et al. 2007).

The Underwater Video Profiler (UVP) was designed and constructed to quantify large (>100 µm) aggregates and zooplankton at the same time in a known volume of water. A principal feature of the instrument is the collection of data at a speed comparable to CTD-based physical, chemical, and optical sensors (i.e., 24Hz). The original UVP and its successor instruments, versions 2 through 4, were large stand-alone packages of nearly 1 m^3 and incorporated a CTD fluorometer and nephelometer (Gorsky et al. 1992; Gorsky et al. 2000). UVP2 and 4 have both been used extensively and have been intercalibrated (Guidi et al. 2007, 2009). UVP4 continues to be used for the assessment of a global distribution of mesopelagic macrozooplankton (Stemmann et al. 2008c). The latest version, UVP5, the instrument described herein, is a miniaturized instrument that can be mounted on a standard rosette frame and interfaced with the CTD. The distributions of particles are displayed together with the CTD data in real time to permit the sampling of particles using Niskin bottles.

Herein, we describe the UVP5 design and calibrations and present experimental results from the BOUM trans-Mediterranean cruise performed within the framework of the SESAME European project (www.sesame-ip.eu).

Materials and procedures

The previous versions of UVP (2 to 4) have produced a database of more than 1300 inter-calibrated profiles since 1991 when they started to be deployed routinely. These instruments required dedicated winch time and their maximum operating depth was 1000 m. The total weight of the UVP4 was 250 kg in air. Battery life was set by the high power consumption of both the lighting systems and the integrated electronics. Image acquisition was not possible at near surface depths during daytime due to light saturation. Furthermore, the overall complexity of the UVP required an onboard technician which further limited widespread use by the oceanographic community. The UVP5 was designed to address these past limitations. Currently, UVP5 can be used for short- or long-term deployments as either an autonomous system (Fig. 1A) or as a specialized CTD sensor (Fig. 1B). The UVP5 can also be incorporated into an autonomous underwater vehicle (AUV), a remotely operated vehicle (ROV), or a drifting or geostationary mooring.

Technical description—The UVP5 weighs less than 30 kg in air and is pressure rated to 3000 m depth. The instrument package contains an intelligent camera, lens, pressure and angle sensors, acquisition and piloting board, internet switch, hard drive, and dedicated electronic power boards. The collimated illumination is delivered by red light-emitting diodes (LEDs) of 625 nm wavelength (Fig. 1C).

The camera (Sony XCI SX1 CCD B&W) has a resolution of 1.3 Megapixel. It has a theoretical 15 Hz acquisition rate and 8 Gb of memory storage, enough for more than 100 profiles in mixed acquisition mode (*see* below). The camera housing con-

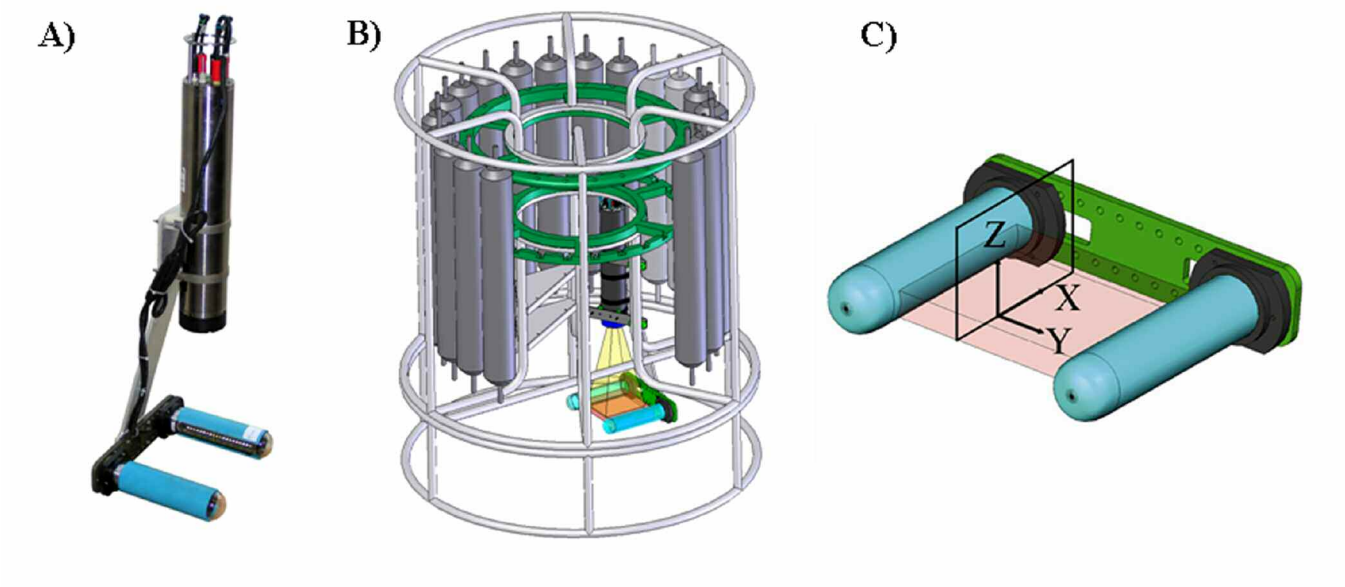

Fig. 1. (A) UVP alone, (B) UVP mounted on a 24-place Niskin bottle rosette frame, (C) schematic diagram of the Underwater Vision Profiler light system and illuminated volume of water (in pink). The recorded image is one portion of this zone (as drawn in 1B).

tains a processor (x86 AMD Geode GX533, 400 Mhz CPU) operated by Windows XP, Ethernet (10/100 TCPIP), a serial and USB interface, and digital input/outputs. Its capability to connect with a keyboard and a monitor allows easy image acquisition and display. Its low acquisition/process power consumption allows long-term data processing using only battery power. The camera is equipped with a 9 mm fixed focal lens (HF9HA-1B Fujinon) to image a 22 × 18 cm field-of-view at a distance of 40 cm from the glass port. The lens is adjusted to obtain focused images in the whole depth of field with sufficient intensity for the camera CCD array. A narrow band pass filter centered on 625 nm (Edmund Optics NT48-087) is positioned in front of the lens to remove the ambient light and keep only the objects illuminated by the UVP red LEDs. This feature allows data acquisition even in sunlit surface waters.

The UVP5 is piloted by a system (Persistor CF2) that allows very low power consumption during sleep mode for long-term deployments. The CF2 board also facilitates communication between operator and camera via RS232, analog to digital conversion for external sensors, digital to analog output to CTD, piloting, energy monitoring, and pressure measurement. An Ethernet switch (Harting econ2000 3x) permits image and data extraction by user and connection with an optional external hard drive that can be inside an AUV, an ROV, or a deep water observatory. Inside the UVP5 pressure case, an optional network drive (LaCie NAS) allows the storage of up to 90 Gb of data and images. This hard drive can be disabled to improve the battery life of the system. The pressure is measured by a 300 bar rated digital sensor (Keller XF33x) having 0.01% accuracy. Two custom-built electronic boards complete the system. The first board is dedicated to power management through DC/DC converters and relays. The second contains the digital/analog (DA) converter, the angle sensor, and an internal temperature sensor (ADIS 16203). The RS232 interfacing from CF2 and input/output are also included on the second board.

A rechargeable lithium-ion 6.3 A/29 V battery pack powers the whole system allowing 7 h recording using the internal hard drive or 14 h using only the camera flash memory. The battery of the CF2 board allows more than 1 y standby with time programmed acquisition sequences of up to 14 h recording on the internal battery. The battery can be charged up to 80% in less than 2 h with a standard charger. The battery voltage is continuously monitored during acquisition periods to prevent loss of data in case of any voltage loss.

The two lighting systems are housed in independent glass cylinders of 60 mm internal diameter and 5 mm thickness. 42 red LEDs (SEOUL × 10491 625 nm) are set behind two polycarbonate semicylindrical lenses. The LEDs are driven by an electronic set-up providing pulsed current of up to 5 A. The typical flash duration is 100 µs to prevent image blur allowing acquisition at deployment speeds up to 1.5 m s^{-1}. Two lighting units are fixed on an aluminum plate facing each other to allow a better light homogeneity in the field of view (FOV) of the camera. The typical light beam is 3 × 20 cm, and its precise measurement is described below. The LEDs are controlled by and synchronized with the camera shutter. The red light was chosen to reduce zooplankton phototactic behavior and to prevent contamination by the sunlight at the surface. The lighting units have sufficient power to allow the Sony camera to record good quality images with a midrange gain of 6 and a linear acquisition look-up table (LUT) leading to very low image noise.

Instrument pilot—Software monitoring the system status and communications with both user and camera runs the CF2 acquisition board. The software is coded in C++ and can be externally updated through a RS232 link to allow change. Acquisition and process sequences can be initiated by the user or an intermediary, such as ROV or AUV, through either the RS232 or an external switch. Sequences can also be started by preset time with a very low power consumption sleeping mode between the sequences. Thousands of time-programmed sequences can be implemented, allowing very long deployments on moorings. An intelligent depth-controlled mode facilitates integration with a CTD without need of any operator onboard to initiate data acquisition. The software also monitors data from up to 7 analogue sensors and sends them to the camera along with the pressure (depth) to be interfaced with the images in real time. The voltage and temperature are also monitored, and the camera acquisition and processing are stopped in case of power loss or overheating. The CF2 board converts summarized data from the images sent by the camera to the DA converter for real time display. It also sends more detailed data through RS232 if a serial link is available. An event logger records all the commands received and sent by the CF2 to help diagnose any technical problem. The whole system can be parameterized through RS232 command without any need to open the pressure case.

Real time image processing—Dedicated software is implemented in the UVP5 intelligent camera. This software acquires and processes images in real time according to settings provided in two initialization files. Here, the gain, shutter, and trigger for the LED pulses are controlled and a background image can be removed. Four modes of operation are provided to adapt the system to users' needs. These modes are (1) full process, (2) image acquisition only, (3) mixed process, and (4) process only. In the full process mode, all images are saved and processed in real time, limiting the acquisition to 3 Hz. In the image acquisition only mode, the images are recorded on the flash memory or the hard drive providing up to 3.5 Hz. In the mixed process mode, the images are acquired and processed to get size and gray level for each object. Vignette images or full images of objects above a preset size limit are saved on the flash memory or the hard drive. This mode saves memory, keeps images of "interesting targets" to be identified later, and allows a rate up to 5.5 Hz. Finally, in process only mode, the images are processed, and only the size and mean gray value of each of the detected objects is saved in a text file. This latter mode is the fastest, and can achieve 6 Hz rate.

The environmental data acquired by the CF2 are saved in text files with the measurements from the objects and some summarized data sent back to the CF2 through RS232 to be transmitted to the user via RS232 or by analogue transmission to the CTD. These data include the number of particles between user-defined size limits, their mean size and gray level, and the same measurements for the organisms larger than the preset size limit.

Image post-processing—A dedicated toolbox (Zooprocess software) has been developed and is publicly available (http://www.zooscan.com, Gorsky et al. 2010). The software allows metadata acquisition and the processing of the images. The regions of interest (ROI) containing interesting objects are extracted as enhanced, size-scaled vignettes. In addition, the number and depth of the recorded source image is appended. A Plankton Identifier Data (http://www.obs-vlfr.fr/~gaspari/Plankton_Identifier/index.php) file (PID) is created containing the variables of every object and the corresponding water depth. Prediction of the most representative categories of organisms is done in Plankton Identifier using the Random Forest method (Breiman 2001). Following initial identification, vignettes are automatically copied into the prediction folders and the identification is validated by taxonomic experts. The validated identifications are then uploaded into the PID files for further analyses. All metadata information, particle measurements, and object identifications are loaded with the available data into a single Matlab standardized database facilitating further the data processing, merging of data from different UVP versions, and rapid printout of particles and zooplankton.

Application in the field—UVP5 was first used intensively during the BOUM experiment (http://www.com.univ-mrs.fr/BOUM/) in June and July 2008. The cruise consisted on an east-to-west transect across the Mediterranean Sea. The project aimed to give a longitudinal description of the biogeochemistry and biological diversity of the Mediterranean Sea, and to produce a detailed study of the biological production in three oligotrophic sites. Initial results of all particles at the three sites and three zooplankton categories at the western site are presented in Figs. 7 to 9. A more detailed analysis and interpretation will be published elsewhere.

The UVP5 was mounted on a 24-bottle rosette (Fig. 1B) and 185 vertical profiles were obtained. All the particles larger than 105 µm were processed and the vignettes of the 18300 objects larger than 600 µm have been extracted using the mixed process mode. A subset of those objects (1000 objects) has been sorted manually to prepare a learning set for automatic image recognition. The Random Forest algorithm was used to pre-sort the objects into 10 categories that have then been further divided into 35 categories based on expert taxonomic analyses.

Assessment

Because the settings for the detection and analysis of particles vary among the different UVP designs, each version must be independently calibrated. The calibration follows two critical steps: (1) calibration of the water volume for a single image and (2) calibration of the size of particle within the image. Particle enumeration is very sensitive to step 1, whereas particle sizing depends on step 2. Both steps are described below. In addition, the performance of the latest UVP version (UVP5) is compared to UVP4 in order to evaluate the possibility of combining data from various UVP versions.

Calibration of image volume—The image volume calibration was performed independently for each of the two lights using an aquarium filled with seawater. The light source illuminated a white calibration sheet and a digital camera recorded images of the calibration sheet using the same manual settings for each of the two lights. To facilitate the acquisition of the calibration images, the continuous illumination mode was used. To reproduce the pulsing mode for the volume calibration, we normalized the light by the highest intensity delivered by each of the two light sources for the 9 independent images.

The center of the image was arbitrarily set as the 0 reference point and images were acquired at –8, –6, –4, –2, 0, 2, 4, 6, 8 cm from the center. Fig. 2A represents the light intensity field along the illuminated volume of water. Each image is the composite of normalized images from the right and left light sources. Fig. 2B corresponds to the light spectrum for an image at –8 cm from the center of the light field. The relative light intensity increases abruptly then reaches a plateau followed by a sharp decrease. The shape of the illumination spectrum indicates that the light field is well defined and that the diffusion on the border of the field is minimal. The same analysis was performed on each image and the light field was reconstructed by linear interpolation between the images (Fig. 2C). To calculate the volume recorded by the UVP5, we chose a light intensity level (threshold) below which the reflection on objects is considered negligible. Fig. 2D shows the variation of the calculated volume as a function of the selected threshold (red curve). The volume decreases while the threshold increases. We employed a mathematical approach to find the best threshold using the derivative of the volume as a function of the threshold. The optimal threshold would be the one for a derivative equal to zero which equates to the situation where there is no variation of the volume as a function of the threshold. The black curve (Fig. 2D) is the approximate derivative of the volume (Y_i-Y_{i+1}), and the green curve corresponds to the moving average with smoothing window selected when the autocorrelation function crosses zero. The optimal threshold is the one for which the smoothing average is a maximum, between 0.5 and 1.5.

The results of this empirical analysis indicates that the optimal threshold is equal to 1 (Fig. 2B and D), a value that equates to a water volume of 1.02 L for each image recorded by the UVP (yellow layer on Fig. 2C).

Calibration of pixel to millimeter conversion—The UVP5 converts the measured area to equivalent spherical diameter (ESD) to estimate the particle size (Jennings and Parlslow 1988). The

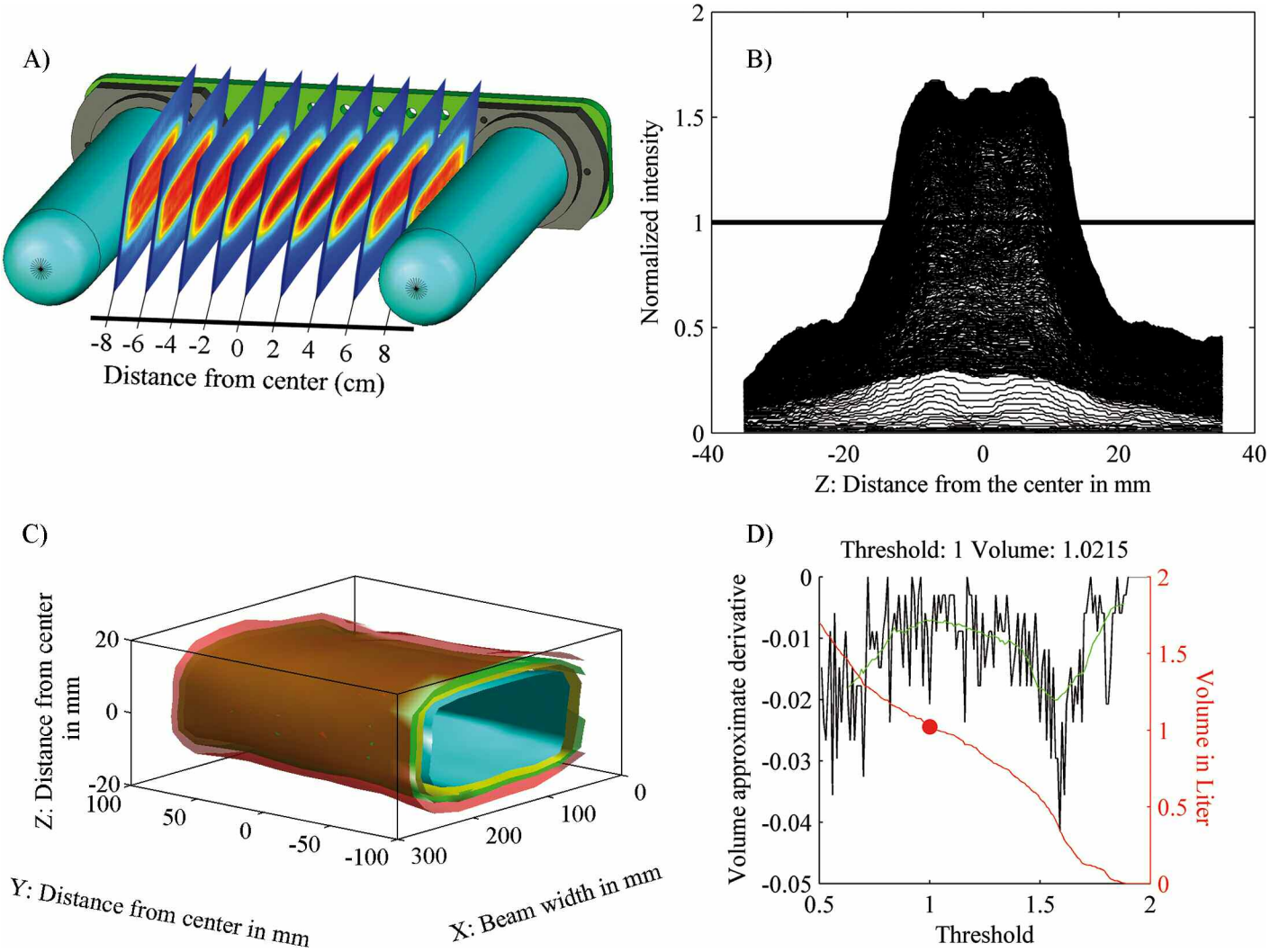

Fig. 2. Reconstruction of the volume of water recorded by the UVP. (A) Repositioning of the 9 images captured in the seawater tank inside the light beam. (B) Light intensity spectrum of the –8 cm image (Fig. 2A) from the center of the light field (*X* axis corresponds to *Z* axis on Fig. 1C). The continuous line represents the threshold 1, which is used to calculate the recorded volume. (C) Reconstruction of the recorded volume using different thresholds; threshold 1 in yellow. (D) Estimation of the recorded volume in function of thresholds values in red. The red point indicates the volume for threshold selected for the UVP5. The green curve is the average of the volume approximate derivative.

objective of the size calibration was to define the equation allowing for the conversion from pixel area of particles recorded by the UVP5 to size. Due to light scatter in the water between the particle and the CCD image, the physical pixel border length of 174 µm cannot be used for small targets (Fig. 3A), and relationships between area in pixels and area in metric units is not linear. However, the pixel size of 174 µm can be used to scale the images of large zooplankton (>600 µm) extracted by the UVP5 software and analyzed in Zooprocess. As the main purpose of the UVP5 is to count and size objects of different origins, we have decided to calibrate size on diverse targets sorted into three major qualitative optical groups (dark, transparent, and heterogeneous). The final curve is computed from the actual area of the selected targets and their pixel surface using the UVP5 images.

The UVP5 was placed horizontally in an experimental water tank filled with filtered (<1 µm) seawater. Zooplankton and particles (individual particles and aggregates) for this calibration experiment were collected in the Bay of Villefranche using both 53-µm and 500-µm mesh nets. The samples were placed in a cold room until processed. Actively swimming zooplankton were killed and preserved with a drop of formaldehyde. All objects were photographed with a Nikon digital camera installed on a Leica stereomicroscope and processed using ImageJ software to determine size (Abramoff et al. 2004; Rasband 1997-2005). About 150 objects were introduced one by one using a pipette into the middle top of the UVP5 field of view. Several images of each object were recorded and processed in real time by the UVP5 to compute particle area. To validate the UVP5 software, we compared each image processed by the UVP5 and by ImageJ software.

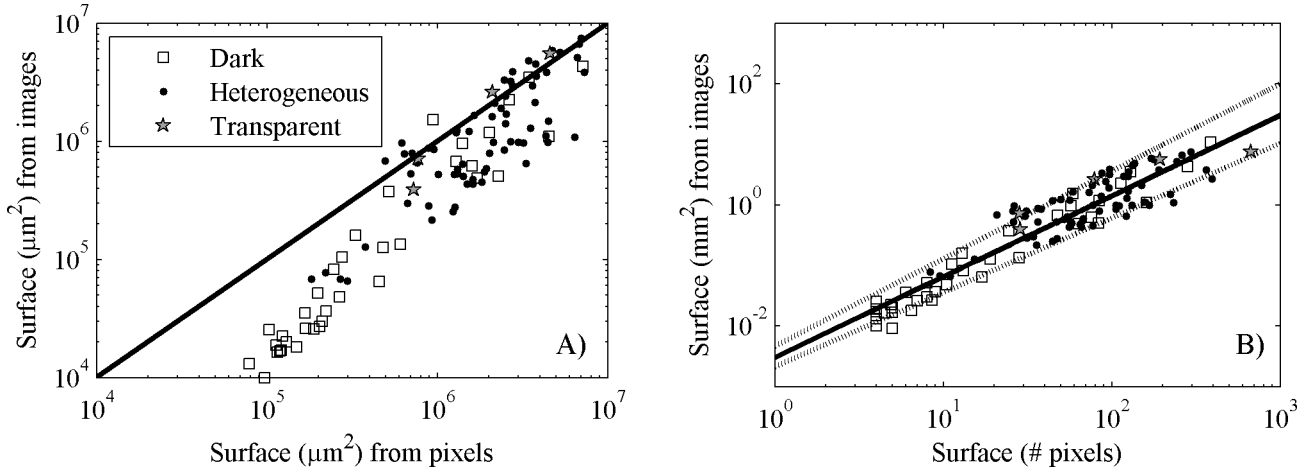

Fig. 3. Surface in pixels compared to surface in metric units for 115 natural objects. (A) Surface in pixels converted to surface in μm² using the pixel size of 174 μm. The continuous line corresponds to the 1:1 ratio. (B) Surface in pixels (S_p) converted to surface in mm² (S_m) using the nonlinear relationship ([insert graphic]) between the two measurements. The continuous line corresponds to the model and dashed lines to the 25 and 75 percentiles for both *A* and *B*.

Control images were acquired in the experimental water tank in ambient light and in the dark. We did not observe any change in the background under these conditions. The background remained completely black demonstrating that only the introduced particles were recorded and analyzed.

The coordinates of each particle sinking in the field of view were plotted to avoid confusion and contamination with any non-introduced particles. A total of 115 objects were finally used in the calibration experiment.

The surface area in pixels (S_p) from an object imaged by the UVP5 was converted into surface area in mm² (S_m) using the following non-linear relationship (Fig. 3B):

$$S_m = A.S_p^B \quad (1)$$

where *A* and *B* are constants. We used the Matlab function *fminsearch* (The Mathworks) to find the values of *A* and *B* minimizing the log-transformed differences (ΔS) between the surface areas for the same particles calculated from the binocular pictures and ImageJ (S_m):

$$\Delta S = \sum_i \left[\log\left(S_{p,i}\right) - \log\left(S_{m,i}\right)\right]^2 \quad (2)$$

The logarithmic transformation was used to give equal weight to differences for small and large particles. The minimization procedure yields only one pair of parameter values. We used a jackknife procedure to estimate the errors of the estimates. The minimization was performed on 1000 subsamples one third the size of the original data set and composed of data pairs selected randomly from the original data set. The results provide the frequency distribution of *A* and *B*. The minimization and jackknife procedure yield median values for *A* = 0.003 and *B* = 1.3348 (Fig. 4 and Table 1)

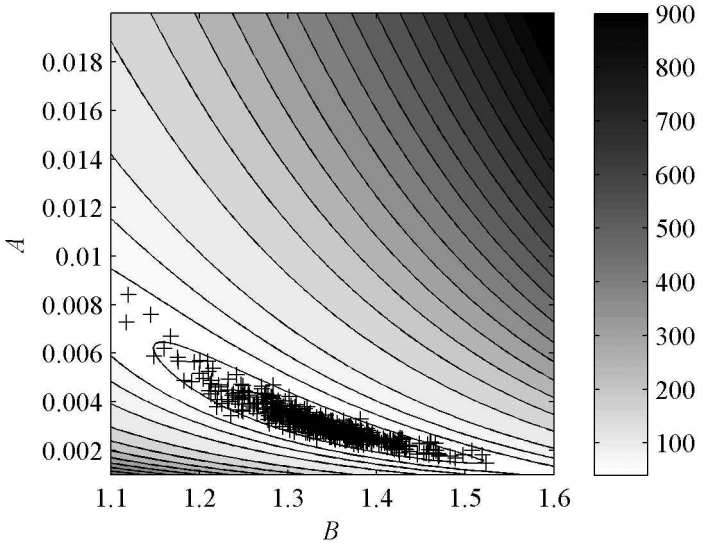

Fig. 4. Residual error ΔS as a function of values of *A* and *B* for the calculus of the particles surface. The best fit values were *A* = 0.0030 and *B* = 1.3348. Darker regions represent greater values for ΔS in mm². The crosses correspond to the values calculated during the jackknife error analysis. The crosses are all located in the area where the residues are the smallest.

Inter-calibration between UVP4 and UVP5—The UVP4 and UVP5 were deployed at approximately the same location and same time during the BOUM cruise in the Mediterranean Sea. Distances between profiles made by the two instruments were less than 2 km and time lags were less than 5 h. During the 2 month cruise, 30 paired profiles were conducted. These profiles allowed comparisons of particle size spectra, total abundances, and slopes of the particles size distribution.

Table 1. Coefficients and exponents of the relationship ($S_m = A.S_p^B$) to convert pixel surface into surface in mm².

A		
Median	Percentile 25	Percentile 75
0.0030	0.0021	0.0047
B		
Median	Percentile 25	Percentile 75
1.3348	1.2298	1.4405

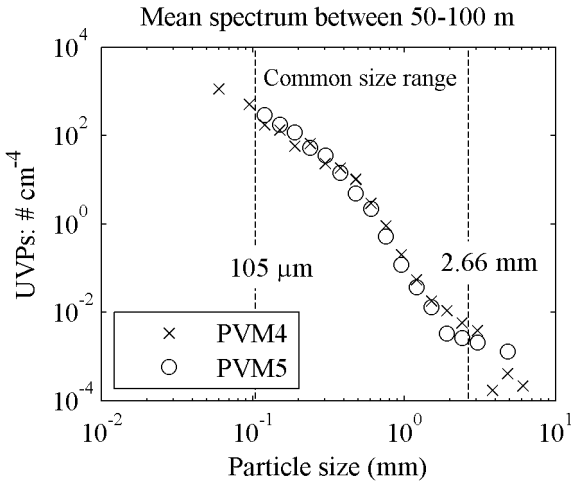

Fig. 5. Mean particle size distribution at the same location and time between 50 and 100 m from both UVP4 and 5 (BOUM experiment). The combined particle size range spans from 105 µm to 2.66 mm.

The two instruments have different fields of view due to the camera properties and the volume of the illumination. The camera resolution limits the detection of small particles, whereas the volume recorded limits the detection of large particles. The larger the volume the higher the chance is to detect sparse large particles. To compare the instruments we need to extract the common size classes for UVP4 and UVP5 (Fig. 5).

The size spectrum of particles ($n = N(s)$) is usually calculated in terms of the concentration (number per unit volume) of particles (ΔC) in a given size range (Δs):

$$n = \Delta C/\Delta s \quad (3)$$

The values of N are very similar from UVP4 and UVP5 considering only particles larger than 105 µm and smaller than 2.66 mm (Fig. 5 and 6A). The Pearson correlation coefficient between measurements from both UVPs is equal to 0.9 ($P < 0.001$) and slope of the regression is equal to 1.01 ($n = 23000$; Fig. 6A). The UVP5 detects more particles per cm^{-4} than UVP4 when their number is less than 10^{-4}. This result is related to the volume of water imaged by the two systems. The UVP5 samples 10 times less volume of water than the UVP4. This difference tends to decrease the probability of correctly estimating the number of particles when this number is small

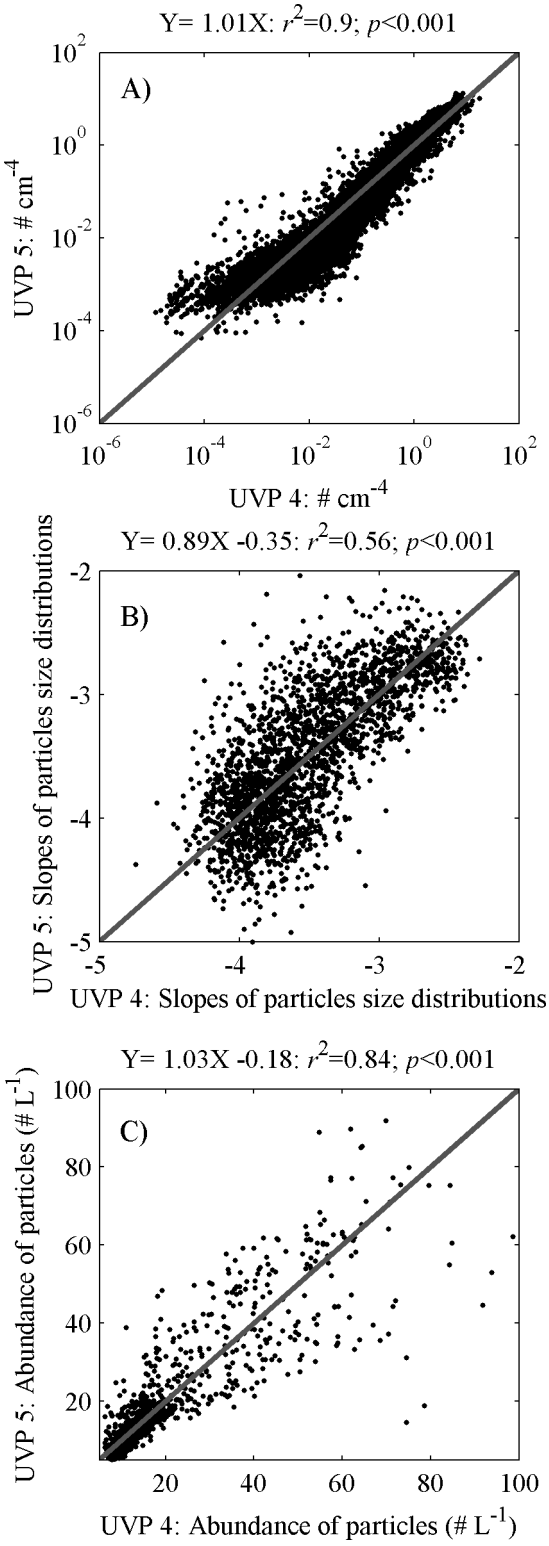

Fig. 6. Comparison between 30 profiles from UVP4 and 5 taking into account the common size range (105 µm to 2.66 mm). (A) Comparison of the number of particles per size classes normalized by the size of the classes. (B) Comparison of the slopes of the size distribution of the particles. (C) Comparison of the abundances of the particles. The continuous lines are 1:1 ratio.

(Jackson et al. 1997; Checkley et al. 2008). This limitation could be compensated by pooling more images from the UVP5 to increase the volume of water analyzed.

Segments of the particle size spectrum frequently fit an expression of the form

$$N = ad^{-b} \quad (4)$$

where a and b are constants, and d is equal to particle diameter (Sheldon et al. 1972; McCave 1984; Jackson et al. 1997). The slope of the Junge-type particle size spectrum is often calculated from $\ln(N) = \ln(a)\text{-}b\ln(d)$ where ln is natural logarithm. The slope (b) is used as the descriptor of the particle size distribution.

Data presented here have not been smoothed, which explains the variations observed on Fig. 6B. However, the Pearson correlation coefficient between calculated slope from UVP4 and UVP5 is significant ($P < 0.001$) and equal to 0.56. The coefficient of the regression between measurements from both instruments is equal 0.89. Data do not deviate significantly from the 1:1 line.

Finally, comparison was done using the abundance of particles between 105 µm and 2.66 mm (Fig. 6C). The coefficient of the regression is not significantly different from 1, and the Pearson correlation coefficient is significant ($P < 0.001$) and equal to 0.84. A small divergence between instruments is observed when the absolute number of particles is less than 10; the UVP5 underestimates the number of particles by a factor of 2 relative to UVP4. This underestimation is a function of the different volumes imaged by the UVP4 and UVP5. As a consequence, even if the results from both UVPs did not differ statistically, comparison of results from both systems needs to be done with caution. The inter-calibration study demonstrates that data from both instruments can be compared in terms of particle size distribution, total abundance, and slope of the distribution.

Examples of particle size and large zooplankton distribution—The vertical profiles of total particle abundance (Fig. 7) acquired at the three major sites of the BOUM experiment show that according to density and fluorescence profiles, the intra-site

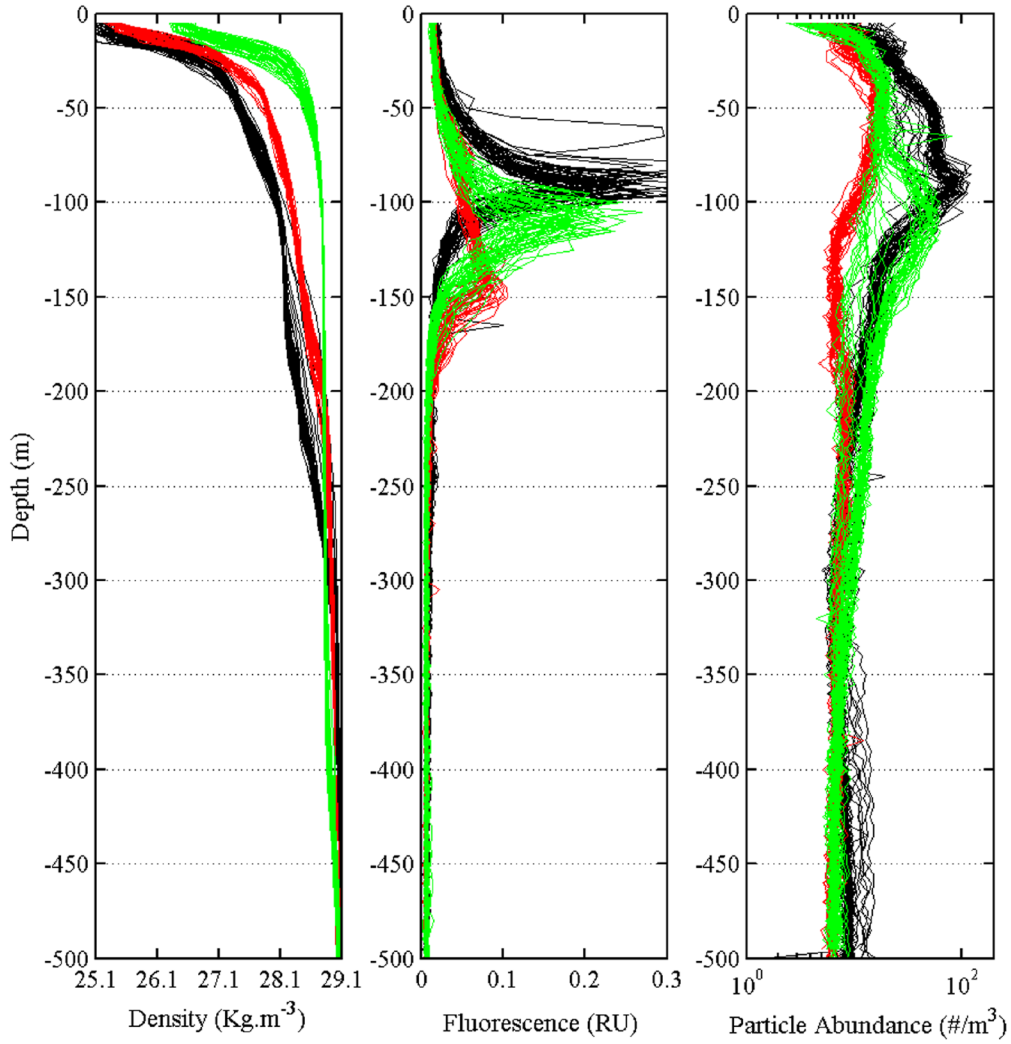

Fig. 7. Vertical distribution of (A) seawater density, (B) fluorescence, and (C) particles > 105 µm in the three locations in the Eastern (site C in green, $n = 31$), Central (site B in red, $n = 28$) and Western (site A in black, $n = 28$) Mediterranean Sea during the BOUM cruise in July 2008.

variability is much lower than the inter-site variability. The UVP5 proved its reliability in counting particles and characterizing the different water masses by their particle content.

The three numerically dominant categories of zooplankton showed distinct vertical patterns with concentrations ranging from 0 to 4 individuals m^{-3} (Figs. 8 and 9). These concentrations are up to 4 orders of magnitude less than particle concentrations (Fig. 7c) and 2 to 3 orders of magnitude less than non-living particles of similar sizes. Large copepods showed a high vertical migration with higher concentrations above 75 m at night (3 organisms m^{-3}) and a more uniform distribution during day time below 100 m. Radiolarians showed a prominent peak (4 organisms m^{-3}) at 75-100 m corresponding to the fluorescence maxima. In contrast, large radiolarians, probably belonging to the Phaedorians, showed a deeper vertical distribution with maxima of approximately 1 organism m^{-3}.

Discussion

The UVP2 documented the export of particles in the Northwestern Mediterranean Sea in relation to seasonal climatic forcing (Gorsky et al. 2002; Stemmann et al. 2002). The UVP3 was a transition version of the family of UVP instruments. The improvements of the optics and illumination in UVP4 enabled simultaneous estimations of the vertical distributions of both particles and zooplankton, and led to the first comparison of mesopelagic macrozooplankton assemblages across oceanic regions (Stemmann et al. 2008c). These assemblages were consistent with epipelagic biogeochemical provinces (Longhurst 1995). In another experiment, the combinations of the 2 systems (UVP2 and UVP4) documented that mesoscale Atlantic eddies spatially constrain the export of particles in different seasons (Guidi et al. 2007). More recently, an analysis of the complete database generated by these instruments shows that the particle size distribution in the mesopelagic layer is closely related to the size distribution of the phytoplankton in the euphotic zone (Guidi et al. 2009).

The particle size distribution can be converted into biomass distribution when assumptions are made about aggregate porosity and density (Stemmann et al. 2008a). Using sediment trap data, Guidi et al. (2008) showed that particle size distribution can also be used to estimate the potential particle settling speed, and hence, mass fluxes in the water column at global scale. This proxy of particle flux serves to detail the vertical resolution of fluxes and estimates the particle remineralization rate that is used in biogeochemical modeling to describe the decrease of the export with depth (Guidi et al. 2009). The UVP5 provides information on particle size distribution at high spatial resolution allowing the description of spatial distribution of carbon flux in different hydrological regimes, frontal zones, gyres, and equatorial systems (Gorsky et al. 2002; Gorsky et al. 2003 Guidi et al. 2007; Stemmann et al. 2008b). The completion of work at high spatial resolution revealed that particle distributions can be constrained in space-inducing heterogeneous export in the open ocean.

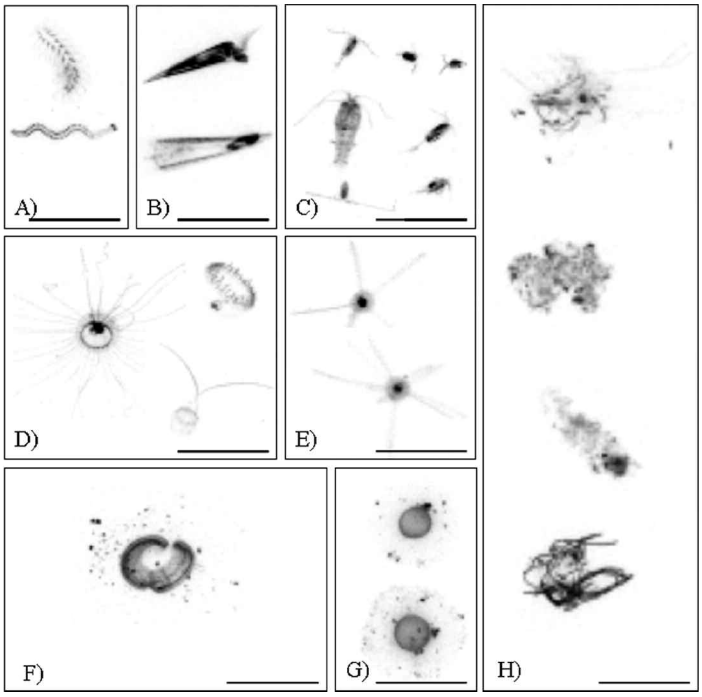

Fig. 8. Zooplankton specimens from the BOUM cruise: (A) annelids, (B) pteropods, (C) copepods, (D) medusas, (E) phaeodarians, (F) appendicularians, (G) radiolarians, and (H) marine aggregates. The black line scale is 5 mm.

Eddies can distribute and export particles that impact the distribution of organisms that feed on settling material (Lampitt et al. 1993; Kiørboe 2000). In addition, macrozooplankton distributions in mesoscale eddies can also be investigated (Stemmann et al. 2008c).

Assessment of spatial variation of particle distribution is as important as the estimation of their temporal variation at one location. The latter will provide information on mechanisms that transform the particles and potentially decrease the carbon export to the mesopelagic layer in specific regions (Stemmann et al. 2004). Seasonal variations of the carbon flux have been observed in the past. These variations have been correlated to the variations of primary production (Karl et al. 1996; Berelson 2001; Boyd and Trull 2007) and to the variations of the phytoplankton community (Boyd and Newton 1999; Stemmann et al. 2002).

The results of the BOUM experiment (Figs. 7–9) demonstrate the ability of the new version of the UVP to provide profiles of the concentration of both aggregates and zooplankton. The current 5 Hz sampling frequency of the mixed process mode and the 1.02 L sampled volume are acceptable for particle estimations in eutrophic conditions. However, for reliable zooplankton estimates in oligotrophic waters, lowering speeds should be reduced, vertical profiles must be replicated, and water volumes sampled should be larger. Higher sampling frequency may be implemented soon taking into account the rapid technological development of the cameras. Because

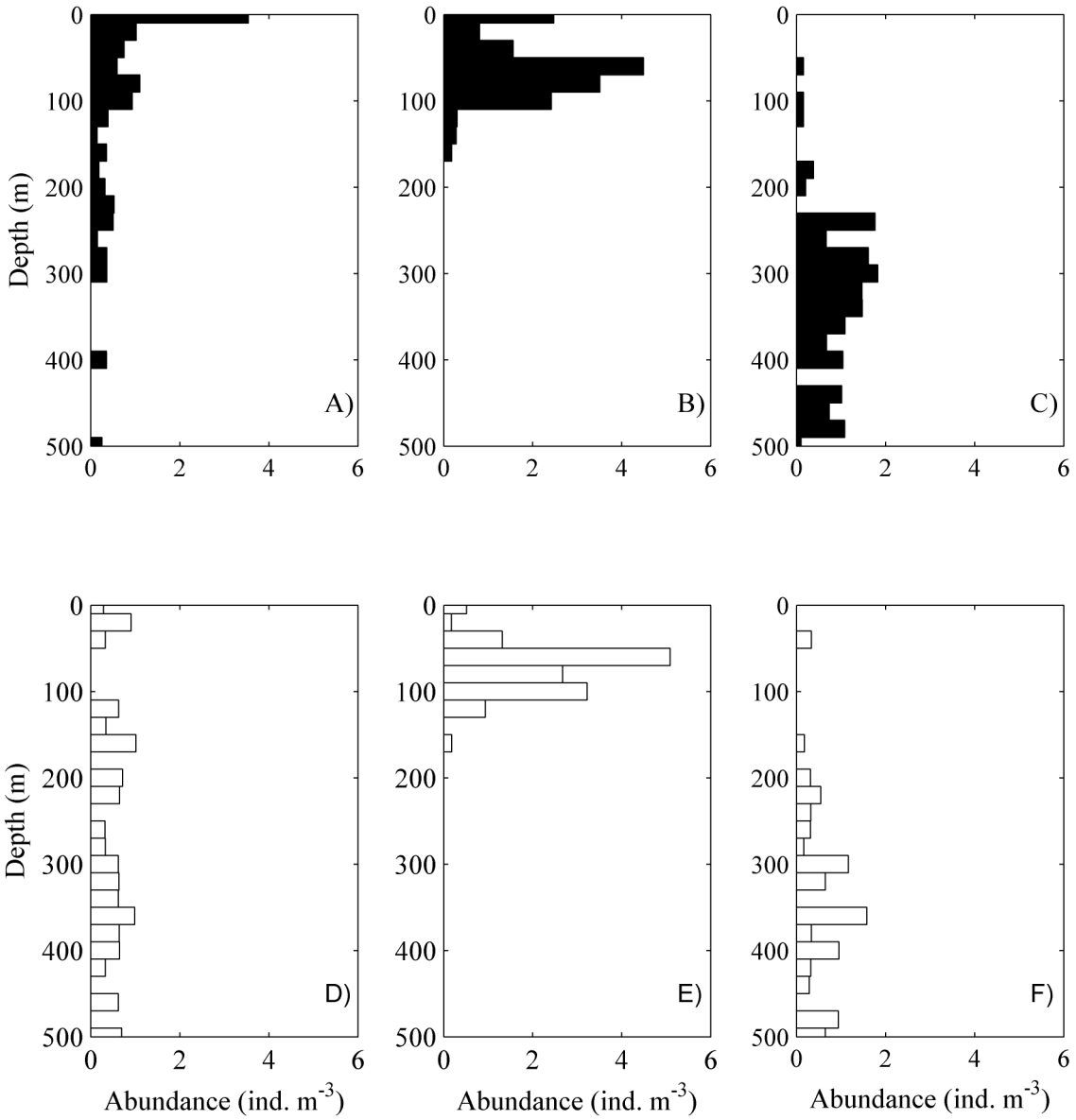

Fig. 9. Vertical distribution of large organisms (> 600 µm) detected by the UVP5 at site A in the Western Mediterranean Sea during the BOUM cruise in July 2008. Copepods (A night, D day), radiolarians (B night, E day) and Phaedorians (C night and F day).

UVP5 can be interfaced with a CTD, the instrument package can be considered as a new sensor for high frequency data acquisition on macroscopic particulate matter and macroplankton distribution especially for investigations in mesopelagic and bathypelagic regimes.

References

Abramoff, M. D., P. J. Magelhaes, and S. J. Ram. 2004. Image processing with ImageJ. Biopho. Inter. 11:36-42.

Alldredge, A. L., and others. 2002. Occurrence and mechanisms of formation of a dramatic thin layer of marine snow in a shallow Pacific fjord. Mar. Ecol. Prog. Ser. 233:1-12 [doi:10.3354/meps233001].

Benfield, M. C., and others. 2007. Rapid research on automated plankton identification. Oceanography 20:172-187.

Berelson, W. M. 2001. The flux of particulate organic carbon into the ocean interior: A comparison of four U.S. JGOFS regional studies. Oceanography 14:59-67.

Boyd, P. W., and P. P. Newton. 1999. Does planktonic community structure determine downward particulate organic carbon flux in different oceanic provinces? Deep-Sea Res. I 46:63-91 [doi:10.1016/S0967-0637(98)00066-1].

———, and T. W. Trull. 2007. Understanding the export of biogenic particles in oceanic waters: Is there consensus? Prog. Oceanogr. 72:276-312 [doi:10.1016/j.pocean.2006.10.007].

Breiman, L. 2001. Random forests. Mach. Learn. 45:5-32 [doi:10.1023/A:1010933404324].

Checkley, D. M., R. E. Davis, A. W. Herman, G. A. Jackson, B. Beanlands, and L. A. Regier. 2008. Assessing plankton and other particles in situ with the SOLOPC. Limnol. Oceanogr. 53:2123-2136.

Cowen, R. K., and C. M. Guigand. 2008. Ichthyoplankton Imaging System (ISIIS): system design and preliminary results. Limnol. Oceanogr. Methods 6:126-132.

Davis, C. S., S. M. Gallager, M. S. Berman, L. R. Haury, and J. R. Strickler. 1992. The Video Plankton Recorder (VPR): Design and initial results. Arch. Hydrobiol. Beih. 36:67-81.

———, F. T. Thwaites, S. M. Gallager, and Q. Hu. 2005. A three-axis fast-tow digital video plankton recorder for rapid surveys of plankton taxa and hydrography. Limnol. Oceanogr. Methods 3:59-74.

Dennett, M. R., D. A. Caron, A. E. Michaels, M. Church, S. M. Gallager, and C. S. Davis. 2002. Video Plankton Recorder reveals high abundance of colonial radiolaria in surface waters of the central north Pacific. J. Plankton Res. 24:797-805 [doi:10.1093/plankt/24.8.797].

Dubelaar, G. B. J., and P. L. Gerritzen. 2000. Cytobuoy: A step forward towards using flow cytometry in operational oceanography. Sci. Mar. 64:255-265.

Gorsky, G., C. Aldorf, M. Kage, M. Picheral, Y. Garcia, and J. Favole. 1992. Vertical distribution of suspended aggregates determined by a new underwater video profiler, p. 275-280. *In* P. Nival, J. Boucher, and M. Bhaud [eds.], 3ème Colloque du Programme National sur le Determinisme du Recrutement, Nantes (France), 1-3 Oct 1991. Annales de l'Institut oceanographique, Paris.

———, M. Picheral, and L. Stemmann. 2000. Use of the Underwater Video Profiler for the study of aggregate dynamics in the North Mediterranean. Estuar. Coast. Shelf Sci. 50:121-128 [doi:10.1006/ecss.1999.0539].

———, L. Prieur, I. Taupier-Letage, L. Stemmann, and M. Picheral. 2002. Large particulate matter in the western Mediterranean I - LPM distribution related to mesoscale hydrodynamics. J. Mar. Syst. 33:289-311 [doi:10.1016/S0924-7963(02)00063-5].

———, R. le Borgne, M. Picheral, and L. Stemmann. 2003. Marine snow latitudinal distribution in the equatorial pacific along 180 degree. J. Geophys. Res. Oceans. 108 [doi:10.1029/2001JC001064].

———, and others. 2010. Digital zooplankton image analysis using the ZooScan integrated system. J. Plankt. Res. 32:285-303.

Guidi, L., L. Stemmann, L. Legendre, M. Picheral, L. Prieur, and G. Gorsky. 2007. Vertical distribution of aggregates (> 110 µm) and mesoscale activity in the northeastern atlantic: Effects on the deep vertical export of surface carbon. Limnol. Oceanogr. 52:7-18.

———, G. A. Jackson, L. Stemmann, J. C. Miquel, M. Picheral, and G. Gorsky. 2008. Relationship between particle size distribution and flux in the mesopelagic zone. Deep-Sea Res. I 55:1364-1374 [doi:10.1016/j.dsr.2008.05.014].

———, and others. 2009. Effects of phytoplankton community on production, size and export of large aggregates: A World-Ocean analysis. Limnol. Oceanogr. 54:1951-1963 [doi:10.4319/lo.2007.52.1.0007].

Herman, A. W., B. Beanlands, and F Phillips. 2004. The next generation of Optical Plankton Counter: the Laser-OPC. J. Plankton Res. 26:1135-1145 [doi:10.1093/plankt/fbh095].

Jackson, G. A., R. Maffione, D. K. Costello, A. L. Alldredge, B. E. Logan, and H. G. Dam. 1997. Particle size spectra between 1 µm and 1 cm at Monterey Bay determined using multiple instruments. Deep-Sea Res. I 44:1739-1767 [doi:10.1016/S0967-0637(97)00029-0].

Jennings, B. R., and K. Parslow. 1988. Particle-size measurement-the equivalent spherical diameter. Proc. Roy. Soc. Lon. A Mat. 419:137-149.

Karl, D. M., J. R. Christian, J. E. Dore, D. V. Hebel, R. M. Letelier, L. M. Tupas, and C. D. Winn. 1996. Seasonal and interannual variability in primary production and particle flux at station ALOHA. Deep-Sea Res. II 43:539-568 [doi:10.1016/0967-0645(96)00002-1].

Karp-Boss, L., L. Azevedo, and E. Boss. 2007. LISST-100 measurements of phytoplankton size distribution: Evaluation of the effects of cell shape. Limnol. Oceanogr. Methods 5:396-406.

Kiørboe, T. 2000. Colonization of marine snow aggregates by invertebrate zooplankton: Abundance, scaling, and possible role. Limnol. Oceanogr. 45:479-484 [doi:10.4319/lo.2000.45.2.0479].

Lampitt, R. S., K. F. Wishner, C. M. Turley, and M. V. Angel. 1993. Marine snow studies in the northeast atlantic ocean: Distribution, composition and role as a food source for migrating plankton. Mar. Biol. 116:689-702 [doi:10.1007/BF00355486].

Longhurst, A. 1995. Seasonal cycles of pelagic production and consumption. Prog. Oceanogr. 36:77-167 [doi:10.1016/0079-6611(95)00015-1].

McCave, I. N. 1984. Size spectra and aggregation of suspended particles in the deep ocean. Deep-Sea Res. I 31:329-352 [doi:10.1016/0198-0149(84)90088-8].

Rasband, W. S. 1997-2005. ImageJ. U. S. National Institutes of Health. <http://rsb.info.nih.gov/ij/>.

Samson, S., T. Hopkins, A. Remsen, L. Langebrake, T. Sutton, and J. Patten. 2001. A system for high resolution zooplankton imaging. IEEE J. Oceanic Eng. 26:671-676 [doi:10.1109/48.972110].

Sheldon, R. W., A. Prakash, and W. H. Sutcliff. 1972. Size distribution of particles in ocean. Limnol. Oceanogr. 17:327-340 [doi:10.4319/lo.1972.17.3.0327].

Sieracki, C. K., M. E. Sieracki, and C. S. Yentsch. 1998. An imaging in-flow system for automated analysis of marine microphytoplankton. Mar. Ecol. Prog. Ser. 168:285-296 [doi:10.3354/meps168285].

Stemmann, L., Eloire, D., Sciandra, A., Jackson, G.A., Guidi, L., Picheral, M., Gorsky, G., 2008a. Volume distribution for particles between 3.5 to 2000 μm in the upper 200 m region of the South Pacific Gyre. Biogeosciences 5, 299-310 [doi:10.5194/bg-5-299-2008].

Stemmann, L., G. Gorsky, J. C. Marty, M. Picheral, and J. C. Miquel. 2002. Four-year study of large-particle vertical distribution (0-1000 m) in the nw mediterranean in relation to hydrology, phytoplankton, and vertical flux. Deep-Sea Res. II 49:2143-2162 [doi:10.1016/S0967-0645(02)00032-2].

———, G. A. Jackson, and D. Ianson. 2004. A vertical model of particle size distributions and fluxes in the midwater column that includes biological and physical processes - part i: Model formulation. Deep-Sea Res. I 51:865-884 [doi:10.1016/j.dsr.2004.03.001].

———, L. Prieur, L. Legendre, I. Taupier-Letage, M. Picheral, L. Guidi, and G. Gorsky. 2008b. Effects of frontal processes on marine aggregate dynamics and fluxes: An interannual study in a permanent geostrophic front (NW Mediterranean). J. Mar. Syst. 70:1-20 [doi:10.1016/j.jmarsys.2007.02.014].

———, and others. 2008c. Global zoogeography of fragile macrozooplankton in the upper 100-1000 m inferred from the underwater video profiler. ICES J. Mar. Sci. 65:433-442 [doi:10.1093/icesjms/fsn010].

Submitted 9 July 2009
Revised 18 May 2010
Accepted 9 July 2010